IL NUOVO CIMENTO Vol. 34 C, N. 5 Suppl. 1 Settembre-Ottobre 2011
DOI 10.1393/ncc/i2011-11000-3

Colloquia: LC10

First results from ALICE

V. Muccifora for the ALICE Collaboration
INFN, Laboratori Nazionali di Frascati - 00044 Frascati (RM), Italy

(ricevuto il 20 Luglio 2011; pubblicato online il 6 Ottobre 2011)

Summary. — The Large Hadron Collider provides p-p and Pb-Pb collisions at the highest centre-of-mass energies to date, which allow to study high-p_T particle, jet and heavy-quark properties in a new energy regime. We present first results from both p-p and Pb-Pb collisions that provide a first characterization of the properties of the matter formed in these collisions.

PACS 25.75.-q – Relativistic heavy-ion collisions.
PACS 25.75.Ld – Collective flow.
PACS 24.10.Nz – Hydrodynamic models.
PACS 12.38.Mh – Quark-gluon plasma.

1. – Introduction

ALICE (A Large Ion Collider Experiment) is the dedicated heavy ion experiment at the CERN LHC, optimised to study matter under extreme conditions of temperature and pressure —the Quark-Gluon Plasma (QGP)— in collisions between heavy nuclei. With an energy up to 30 times higher than RHIC, a very different type of QGP, *e.g.*, in terms of initial temperature, lifetime and system volume is expected as well as an abundance of hard signals like jets and heavy quarks which serve as probes to study QGP properties. Moreover ALICE has several features that make it an important contributor to proton-proton physics at the LHC. Most of heavy-ion observables require p-p measurements of the same observables for comparison. In addition to the benchmark role, the study of p-p collisions in ALICE will also provide a detailed characterisation of global event properties over a range of LHC energies, which will be very useful for tuning Monte Carlo generators to better describe soft and semi-hard QCD processes.

ALICE is a general-purpose experiment whose detectors measure and identify mid-rapidity hadrons, leptons and photons produced in the interaction. A unique design, with very different optimization than the one selected for the dedicated p-p experiments at LHC, has been adopted for ALICE. This results from the requirements to track and identify particles from very low ($\sim 100\,\mathrm{MeV}\,c^{-1}$) up to fairly high ($\sim 100\,\mathrm{GeV}\,c^{-1}$) transverse momentum p_T, to reconstruct short-lived particles such as hyperons, D and B mesons, and to perform these tasks in an environment with large charged-particles

multiplicities. The main design features include a robust and redundant tracking over a limited region of pseudorapidity, designed to cope with the very high particle density of nuclear collisions, a minimum of material in the sensitive tracking volume to reduce multiple scattering, and several detector systems dedicated to particle identification over a large range in momentum. Tracking relies on a set of high-granularity detectors: an Inner Tracking System (ITS) consisting of six layers of silicon detectors, a large-volume Time-Projection Chamber (TPC) and a high granularity Transition-Radiation Detector (TRD). Hadrons, electrons and photons are detected and identified in the central rapidity region ($-0.9 \leq \eta \leq 0.9$) by a complex system of detectors immersed in a moderate (0.5T) magnetic field. Particle detection in the central region is performed by measuring energy loss in the tracking detectors, transition radiation in the TRD, Time Of Flight (TOF) with a high-resolution array, Cherenkov radiation with a High-Momentum Particle Identification Detector (HMPID) and photons with two single-arm electromagnetic calorimeters (high resolution PHOS and large acceptance EMCAL). The forward muon arm ($-4.0 \leq \eta \leq -2.4$) consists of a complex arrangement of absorbers, a large dipole magnet, and 14 stations of tracking and triggering chambers. Several smaller detectors for triggering and multiplicity measurements (ZDC, PMD, FMD, T0, V0) are located at small angles. The layout of the ALICE detector and its different subsystems are described in detail in [1].

The LHC started operating in November 2009 with pp collisions at $\sqrt{s} = 900\,\text{GeV}$ and reached its current maximum energy of 7 TeV in March 2010.

First heavy ion collisions at $\sqrt{s} = 2.76\,\text{TeV}$ per nucleon-nucleon started in November 2010. With a fourteen-fold increase with respect to nucleus-nucleus collisions at RHIC this constitutes the largest energy increase in the heavy-ion physics. LHC worked exceedingly well also for heavy ions, allowing to obtain during the Pb-Pb run and shortly after it, the first physics results.

2. – Results from p-p collisions

The charged particle pseudorapidity density $\mathrm{d}N_{\mathrm{ch}}/\mathrm{d}\eta$ as well as the multiplicity distributions N_{ch} were measured at 0.9, 2.36 and 7 TeV for inelastic and non-single diffractive collisions [2-4]. In fig. 1 (left) the centre-of-mass energy dependence of $\mathrm{d}N_{\mathrm{ch}}/\mathrm{d}\eta$ for charged particles is shown for different event classes. The increase of the pseudorapidity density with increasing centre-of-mass energies is significantly higher than predicted by most event generators. The multiplicity distribution measured at 7 TeV compared to different models is shown in fig. 1 (right). The shape of the measured multiplicity distribution is not reproduced by any of the event generators considered. The discrepancy does not appear to be concentrated in a single region of the distribution, and varies with the model.

Likewise, neither the transverse momentum distribution at 900 GeV nor the dependence of average p_T on N_{ch} is well described by various versions of generators [5] as shown in fig. 2. In particular in the low-p_T region, where the bulk of the particles are produced, the models require further tuning.

The measurement of Bose Einstein (HBT) correlations between identical particle pairs allows to assess the size of the emitting source. These mesurements provide a precision tool in heavy-ion collisions to probe the geometry and the space-time evolution of the dense matter system created in the collisions, however HBT measurements at LHC are important also in p-p as a comparison for the heavy ion data. ALICE measured two-pion correlation functions in pp collisions at $\sqrt{s} = 0.9\,\text{TeV}$ and at $\sqrt{s} = 7\,\text{TeV}$ [6,7]. The

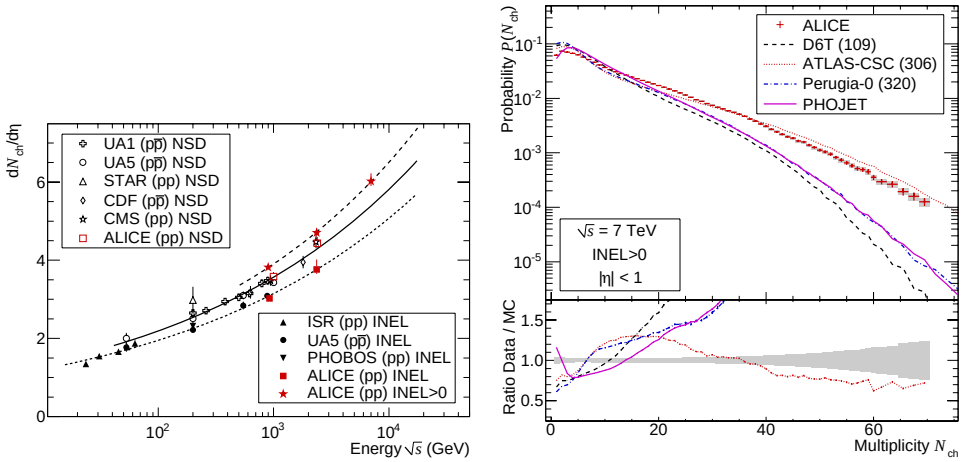

Fig. 1. – Left: charged-particle pseudorapidity density in the central pseudorapidity region $|\eta| < 0.5$ for inelastic and non-single diffractive collisions, and in $|\eta| < 1$ for inelastic collisions with at least one charged particle in that region (INEL$> 0_{|\eta|<1}$), as a function of the centre-of-mass energy. The lines indicate the fit using a power-law dependence on energy. Right: multiplicity distribution at 7 TeV is compared to models. In the lower part, the ratios between the measured values and model calculations are shown. See [4] and references therein.

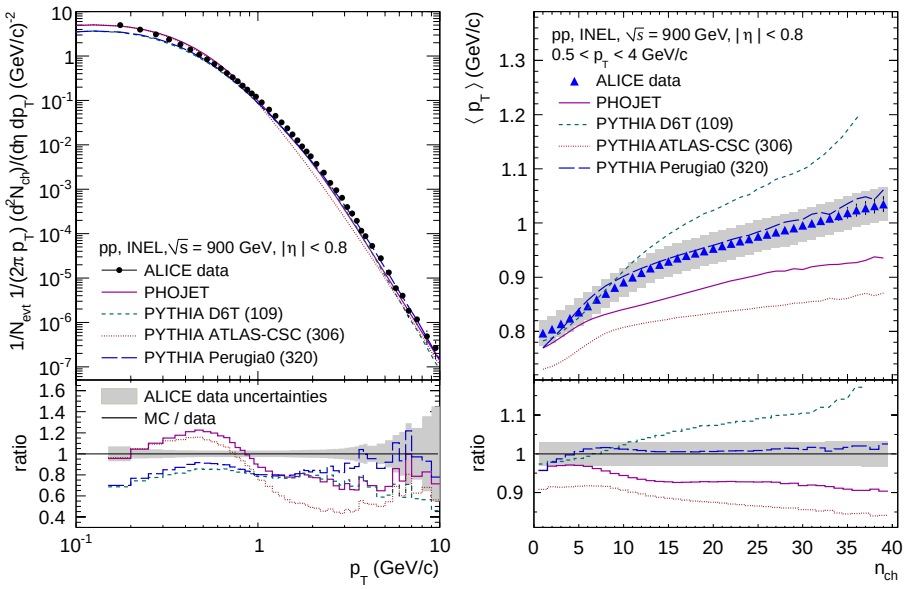

Fig. 2. – Comparison of the primary charged particle differential yield in INEL pp collisions at $\sqrt{s} = 900\,\text{GeV}$ and $|\eta| < 0.8$ (left) and of the average transverse momentum of charged particles for $0.5 < p_T < 4\,\text{GeV}/c$ (right) to results from PHOJET and PYTHIA tunes. In the lower panels, the ratio Monte Carlo over data are shown. See [5] and references therein.

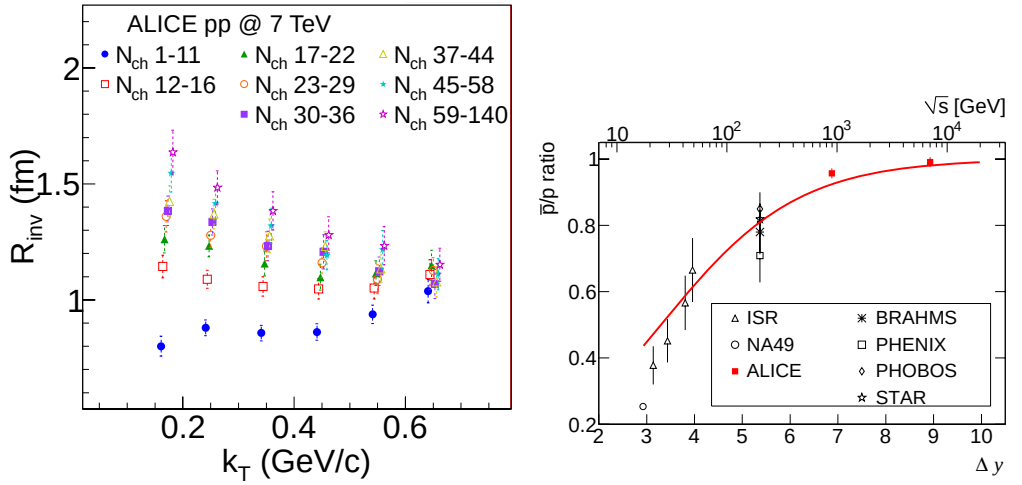

Fig. 3. – Left: 1-dimensional $R_{\rm inv}$ HBT radius for different multiplicity and k_T ranges for the $\sqrt{s} = 7\,\text{TeV}$ data. See [7] and references therein. Right: central rapidity $\overline{\rm p}/{\rm p}$ ratio as a function of the rapidity interval Δy (lower axis) and centre-of-mass energy (upper axis). See [8] and references therein.

analysis was performed in multiplicity and pair transverse momentum $k_T = [p_{T1}+p_{T2}]/2$. HBT radii obtained by 1-dimensional correlation functions are shown in fig. 3 (left) as a function of k_T. The source size increases smoothly with multiplicity, while the decrease with pair momentum becomes significant only for high p-p multiplicities. A detailed comparison in the various HBT radius components (outward, sideward and longitudinal) reveals qualitatively similar trends suggesting the development of space-momentum correlations, at least for collisions producing a high multiplicity of particles.

The LHC opens the possibility to investigate "baryon-number transport" over very large rapidity intervals by measuring the antiproton-to-proton production ratio $R = N_{\overline{\rm p}}/N_{\rm p}$ at midrapidity. Most of the (anti-)protons at midrapidity are created in baryon-antibaryon pair production, implying equal yields. Any excess of protons over antiprotons is therefore associated with the baryon-number transfer from the incoming beam. Model predictions for the ratio R at LHC energies are very close to the unity, with the difference between various models only of the order of a few percent. The measured R as a function of the rapidity loss $\Delta y = y_{\rm beam} - y_{\rm baryon}$, where $y_{\rm beam}(y_{\rm baryon})$ is the rapidity of the incoming beam (out-going baryon), is shown in fig. 3 (right). R was found to be compatible with 1.0 at 7 TeV and 4% below 1.0 at 900 GeV, with an experimental uncertainty of about 1.5%, dominated by the systematic error. These results are consistent with a suppression of the baryon transport over large rapidity intervals in p-p collisions.

Measurements of identified particles at the LHC injection energy and in the low transverse momentum region, along with their comparison with QCD-inspired models, constitute a baseline for comparisons with higher centre-of-mass energies. The production of identified stable charged particle (π, K, p), of mesons containing strange quarks ($\rm K^0_S, \phi$) and doubly strange baryons (Λ, $\overline{\Lambda}$, and $\Xi^- + \overline{\Xi}^+$) are measured at central rapidity in p-p collisions at $\sqrt{s} = 0.9\,\text{TeV}$ [9, 10]. The shapes of the p_T spectra are also compared to PHOJET and several tunes of PYTHIA models. For all species the p_T spectra are found to be slightly harder (*i.e.* they have a slower decrease with p_T) than the models,

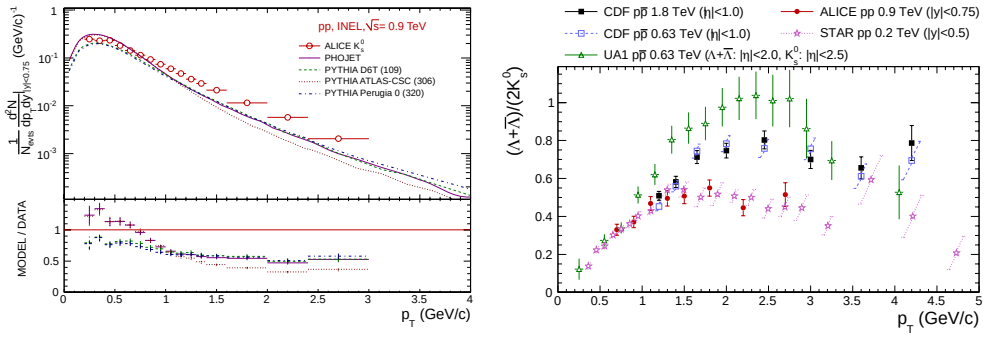

Fig. 4. – Left: comparison of the transverse momentum differential yield for the K^0_S particles for INEL pp collisions with PHOJET and PYTHIA tunes. Right: $(\Lambda + \overline{\Lambda})/2K^0_S$ as a function of p_T for different collision energies in pp and $p\overline{p}$ minimum bias events. See [10] and references therein.

as presented in fig. 4 (left) for K^0_S. For transverse momenta larger than $\sim 1\,\mathrm{GeV}/c$ the strange particle spectra are strongly underestimated by all models, by a factor of ~ 2 for K^0_S and even ~ 3 for hyperons. The discrepancy is smaller in the case of the ϕ.

Baryon-to-meson ratios are of particular interest: the anomalous increase of the baryon-to-meson ratio with centrality observed in nuclear collisions at RHIC, known as "meson-baryon anomaly", has been interpreted as an indirect sign of the QGP. The baryon-to-meson ratio as a function of p_T obtained with the $(\Lambda+\overline{\Lambda})$ and K^0_S spectra measured by ALICE at $\sqrt{s} = 0.9\,\mathrm{TeV}$ is presented in fig. 4 (right). It includes the $(\Lambda+\overline{\Lambda})/2K^0_S$ ratio in pp collisions at 200 GeV measured by STAR, and the ratios in $p\overline{p}$ collisions at 630 GeV and 1800 GeV computed with the $(\Lambda + \overline{\Lambda})$ and K^0_S spectra published by CDF and UA1. The ALICE ratio agrees very well with the STAR results in the measured p_T range, which would suggest little or no energy dependence of $(\Lambda + \overline{\Lambda})/2K^0_S$ ratio. These results provide a useful baseline for comparisons with recent tunes of Monte Carlo and a reference for measurements in heavy-ion collisions at the LHC.

3. – Results from Pb-Pb collisions

A new frontier in the study of QCD matter opened with the first collisions of ^{208}Pb ions in November 2010. These collisions are expected to generate matter at unprecedented temperatures and energy densities in the laboratory. The first step in characterizing the system produced in these collisions is the measurement of the charged-particle pseudo-rapidity density, which constrains the dominant particle production mechanisms and is essential to estimate the initial energy density. The dependence of the charged-particle multiplicity density on energy and system size reflects the interplay between hard parton-parton scattering processes and soft processes. Predictions of models that successfully describe particle production at RHIC vary by a factor of two at the LHC [11, 12]. The value measured at ALICE [13] at mid-rapidity in Pb-Pb collisions at a centre-of-mass energy per nucleon pair $\sqrt{s_{NN}} = 2.76\,\mathrm{TeV}$, $\mathrm{d}N_{\mathrm{ch}}/\mathrm{d}\eta \approx 1600$, represents an increase of about a factor 1.9 relative to p-p collisions at similar collision energies, and about a factor 2.2 to central Au-Au collisions at $\sqrt{s_{NN}} = 0.2\,\mathrm{TeV}$. When combined with lower energy data, the charged-particle pseudo-rapidity density per participant pair, N_{part}, rises stronger with energy than in p-p, approximately with $s^{0.15}$ as shown in fig. 5 (left).

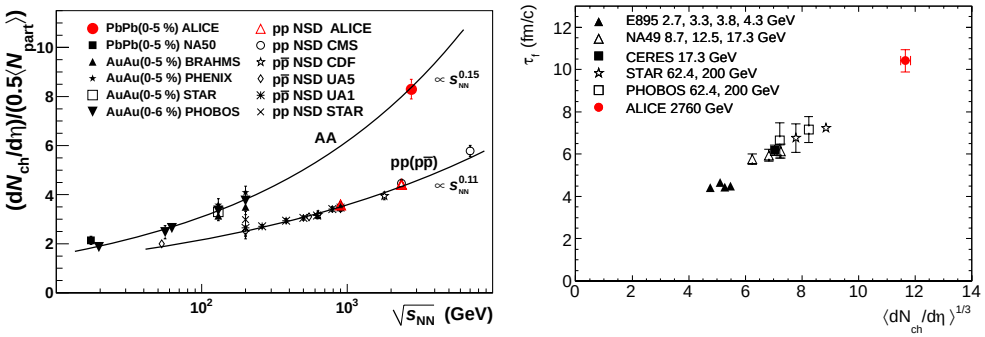

Fig. 5. – Left: charged particle pseudorapidity density per participant pair *vs.* centre-of-mass energy for pp and AA collisions. See [13] and references therein. Right: the decoupling time extracted from $R_{\rm long}(k_T)$. The ALICE result is compared to those obtained for central gold and lead collisions at lower energies. See [17] and references therein.

The centrality dependence of $\mathrm{d}N_{\rm ch}/\mathrm{d}\eta$ has been also measured at ALICE [14] as this observable is important to understand the relative contributions to particle production of hard scattering and soft processes, and may provide insight into the partonic structure of the projectiles. The charged-particle density per participant pair increases with $\langle N_{\rm part}\rangle$, from 4.4±0.4 for the most peripheral to 8.4±0.3 for the most central class. The centrality dependence of the multiplicity is found to be very similar for $\sqrt{s_{_{NN}}} = 2.76\,\mathrm{TeV}$ and $\sqrt{s_{_{NN}}} = 0.2\,\mathrm{TeV}$ for the RHIC experiments [15]. Theoretical descriptions that include a mechanism to moderate the multiplicity evolution with centrality are favoured by the data.

A measurement of elliptic flow v_2, the second Fourier coefficient of the final state hadron azimuthal distribution, at the LHC is a crucial test the validate the hydrodynamic description of the medium and to measure its thermodynamic properties, in particular shear viscosity and the equation of state [11]. $v_2(p_T)$ has been measured at ALICE [16] for various centralities. Comparison with STAR measurements for the same centrality from Au-Au collisions at $\sqrt{s_{_{NN}}} = 200\,\mathrm{GeV}$ shows that the value of $v_2(p_T)$ does not change within uncertainties from $\sqrt{s_{_{NN}}} = 200\,\mathrm{GeV}$ to 2.76 TeV. The observed similarity at RHIC and LHC of p_T-differential elliptic flow at low p_T is consistent with predictions of hydrodynamic models. The p_T integrated elliptic flow however increases compared to RHIC by some 30% for mid-central collisions; hydrodynamic predicts an increased radial flow which implies an increased integrated flow.

While the hydrodynamic approach is rather successful in describing the momentum distributions of hadrons in ultrarelativistic nuclear collisions, the spatial distributions of decoupling hadrons are more difficult to reproduce and thus provide important model constraints on the initial temperature and equation of state of the system. The HBT radii have been extracted from the two-pion correlation functions measurement [17]. The product of the radii, which is connected to the volume of the homogeneity region, shows a linear dependence on the charged-particle pseudorapidity density and is two times larger at the LHC than at RHIC. Within hydrodynamic scenarios, the decoupling time (τ_f) for hadrons at midrapidity has been estimated as shown in fig. 5 (right). As can be seen, τ_f scales with the cube root of charged-particle pseudorapidity density and reaches 10–11 fm/c in central Pb-Pb collisions at $\sqrt{s_{_{NN}}} = 2.76\,\mathrm{TeV}$ which is 40% larger than at RHIC. These results, taken together with those obtained from the study of

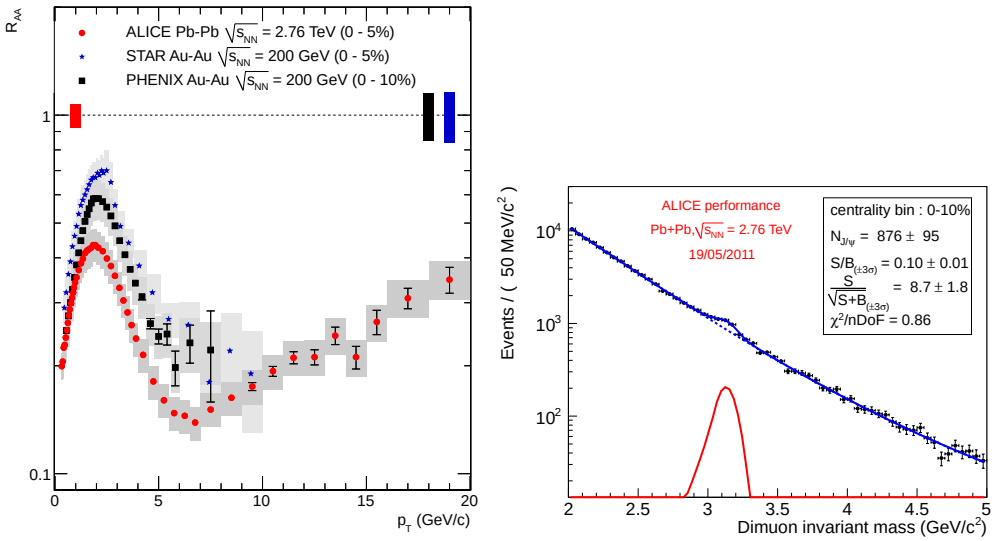

Fig. 6. – Left: nuclear modification factor R_{AA} for central Pb-Pb at LHC compared to RHIC data. See [18] and references therein. Right: $J/\psi \to \mu^+\mu^-$ invariant mass distribution at forward rapidity ($2.5 < y < 4$).

multiplicity [13, 14] and the azimuthal anisotropy [16], indicate that the fireball formed in nuclear collisions at the LHC is hotter, lives longer, and expands to a larger size at freeze-out as compared to lower energies.

To study the full evolution of the produced medium the use of the so-called *hard probes* is of particular interest. While in p-p collisions the partons evolve in the QCD-vacuum and fragment directly into jets of observable hadrons, in heavy-ion collisions scattered partons can lose energy via medium induced gluon radiation or elastic scattering, with the amount of energy loss depending on the color charge and mass of the parton, the traversed path length, and the medium density.

To quantify nuclear medium effect we have measured the primary charged particle p_T spectra and nuclear modification factors R_{AA} in central (0–5%) and peripheral (70–80%) Pb-Pb collisions at $\sqrt{s_{NN}} = 2.76\,\text{TeV}$ [18]. At high p_T, where production from hard processes is expected to dominate, there is a marked difference between peripheral and central events. In peripheral collisions, R_{AA} reaches about 0.7 and shows no pronounced p_T dependence for $p_T > 2\,\text{GeV}/c$, indicating only weak parton energy loss. In central collisions, R_{AA} results are shown in fig. 6 (left) where are compared to measurements of R_{AA} of charged hadrons ($\sqrt{s_{NN}} = 200\,\text{GeV}$) by the PHENIX and STAR experiments [19, 20] at RHIC. In central collisions at the LHC R_{AA} exhibits a very strong suppression, reaching a minimum of ≈ 0.14 at $p_\text{T} = 6$–$7\,\text{GeV}/c$. A significant rise by about a factor of two is observed for $7 < p_\text{T} < 20\,\text{GeV}/c$. Despite the much flatter p_T spectrum in p-p at the LHC, the nuclear modification factor at $p_\text{T} = 6$–$7\,\text{GeV}/c$ is smaller than at RHIC. This suggests an enhanced energy loss and therefore a denser medium at LHC.

Finally, measurements of strange and heavy-flavour particle production have been carried out, as well as studies of jet production and jet-like particle correlations [21]. As an example of the ALICE detector performance during the Pb-Pb run, we report in fig. 6 (right) the invariant mass distribution showing the $J/\psi \to \mu^+\mu^-$ decays in the forward muon spectrometer.

4. – Conclusions

ALICE has measured already during the first year of data taking a comprehensive list of observables in p-p and Pb-Pb collisions. We have presented the first significant results of many observables: particle multiplicities, Bose-Einstein correlations, collective flow, suppression of charged particle production in central Pb-Pb collisions. These measurements provide a first characterization of the hot and dense state of strongly-interacting matter produced in heavy-ion collisions at the LHC energies.

REFERENCES

[1] Aamodt K. *et al.* (ALICE), *J. Instrum.*, **3** (2008) S08002.
[2] Aamodt K. *et al.* (ALICE), *Eur. Phys. J. C*, **65** (2010) 111.
[3] Aamodt K. *et al.* (ALICE), *Eur. Phys. J. C*, **68** (2010) 89.
[4] Aamodt K. *et al.* (ALICE), *Eur. Phys. J. C*, **68** (2010) 345.
[5] Aamodt K. *et al.* (ALICE), *Phys. Lett. B*, **693** (2010) 53.
[6] Aamodt K. *et al.* (ALICE), *Phys. Rev. D*, **82** (2010) 052001.
[7] Aamodt K. *et al.* (ALICE), arXiv:1101.3665 [hep-ex].
[8] Aamodt K. *et al.* (ALICE), *Phys. Rev. Lett.*, **105** (2010) 072002.
[9] Aamodt K. *et al.* (ALICE), arXiv:1101.4110 [hep-ex].
[10] Aamodt K. *et al.* (ALICE), *Eur. J. Phys. C*, **71** (2011) 1594.
[11] Armesto N. *et al.*, *J. Phys. G*, **35** (2008) 054001.
[12] Armesto N., arXiv:0903.1330 [hep-ph].
[13] Aamodt K. *et al.* (ALICE), *Phys. Rev. Lett.*, **105** (2010) 252301.
[14] Aamodt K. *et al.* (ALICE), *Phys. Rev. Lett.*, **106** (2011) 032301.
[15] Adler S. S. *et al.* (PHENIX Collaboration), *Phys. Rev. C*, **71** (2005) 034908 (049901 (Erratum)) [arXiv:nucl-ex/0409015].
[16] Aamodt K. *et al.* (ALICE), *Phys. Rev. Lett.*, **105** (2010) 252302.
[17] Aamodt K. *et al.* (ALICE), *Phys. Lett. B*, **696** (2011) 328.
[18] Aamodt K. *et al.* (ALICE), *Phys. Lett. B*, **696** (2011) 30.
[19] Adler S. S. *et al.* (PHENIX Collaboration), *Phys. Rev. C*, **69** (2004) 034910.
[20] Adams J. *et al.* (STAR Collaboration), *Phys. Rev. Lett.*, **91** (2003) 172302.
[21] *XXII International Conference on Ultra-relativistic Nucleus-Nucleus Collisions (Quark Matter) Annecy (France), May 23–28, 2011*: `http://qm2011.in2p3.fr`.